2010

Building-Integrated Photovoltaic/Thermal Systems – Numerical Prediction of Exterior Convective Heat Transfer Coefficients and Parametric Analysis

Chowdhury Mohammad Jubayer
Department of Mechanical and Materials Engineering

Panagiota Karava
Purdue University

Eric Savory
Department of Mechanical and Materials Engineering

Building-integrated Photovoltaic/Thermal systems – numerical prediction of exterior convective heat transfer coefficients and parametric analysis

Chowdhury Mohammad JUBAYER[1], Panagiota KARAVA[2]*, Eric SAVORY[3]

[1]The University of Western Ontario, Department of Mechanical and Materials Engineering,
London, Ontario, Canada
Contact Information (+1-519-661-2111 Ext. 88146, +1-519-661-3339, cjubayer@uwo.ca)

[2]Purdue University, School of Civil Engineering and Division of Construction Engineering and Management,
West Lafayette, Indiana, USA
Contact Information (+1-765-494-4573, +1-765-494-0644, pkarava@purdue.edu)

[3]The University of Western Ontario, Department of Mechanical and Materials Engineering,
London, Ontario, Canada
Contact Information (+1-519-661-2111 Ext. 88256, +1-519-661-3020, esavory@eng.uwo.ca)

* Corresponding Author

ABSTRACT

The wind-induced exterior convective heat transfer coefficients (CHTC) for a photovoltaic/thermal (PV/T) system mounted on the windward 30° roof slope of a low-rise building have been computed using high resolution 3-D steady RANS with the Realizable k-ε (R k-ε) and the Shear Stress Transport k-ω (SST k-ω) turbulence models, as well as unsteady RANS with the SST k- ω turbulence closure. For validation purposes a 1:50 scale model of the building, with full-scale plan dimension of 4.2 m x 6 m and a 3 m roof height, was tested in a boundary layer wind tunnel. Results for the wind direction normal to the eaves show that the SST k-ω turbulence closure performed better than the R k-ε model in terms of matching the model-scale wind tunnel velocity profiles over the windward roof. A parametric analysis has been performed for different Reynolds numbers ($1.3x10^5$ to $7.7x10^5$), based on wind speed at eaves height and roof length, using the SST k- ω turbulence model. A correlation has been developed for exterior CHTC, using dimensionless parameters, and compared with results from previous full-scale experiments as well as with boundary layer theory.

1. INTRODUCTION

A Building Integrated Photovoltaic/Thermal system (BIPV/T) consists of a photovoltaic array installed as an essential component of the building envelope (typically a façade or a roof). In this system, the circulation of a fluid (usually air) in a channel underneath the PV panels, permits recovery of a significant portion of the incident solar radiation as thermal energy. Thus, BIPV/T systems produce both electricity and heat. However, several details of these innovative systems could benefit from further investigation. For example, full-scale experimental data (Candanedo *et al.*, 2010; Chen, 2009) for a BIPV/T system installed in a house show that 30-50% of the absorbed solar energy is removed by wind-induced external convective heat transfer. Thus, accurate prediction of exterior CHTC is essential for optimizing BIPV/T systems. The exterior CHTC relates the heat flux normal to the PV panel to the difference between the surface temperature of the PV and a reference temperature, which is generally the temperature of the outside environment, $h = q_{PV} / (T_{PV} - T_{ref})$, where, h = CHTC ($W/m^2$-K); q_{PV} = heat flux normal

to the PV surface (W/m^2); T_{PV} = temperature of the PV Panel (K); T_{ref}, = reference temperature (K), such that T = T_{PV} - T_{ref}.

Previous work on CHTC has considered geometries in four main categories: wall-mounted flat and inclined plates, wall-mounted cubes, roof-mounted solar collectors, and building surfaces, including both experimental (wind tunnel, full-scale) and CFD studies. In most cases, research was undertaken to establish relationships between h (W/m^2-K) and a reference air velocity V (m/s) for different plane surfaces, sometimes presented in non-dimensional form. Table 1 summarizes correlations developed for geometries relevant to this work, e.g. inclined plates, solar collectors, and building surfaces. A recent overview of wind convection coefficient correlations has been provided by Palyvos (2008) while an interesting discussion on discrepancies in previous findings can be found in Blocken *et al.* (2009).

Table 1 Relationships between CHTC (h) and wind velocity (V) or Reynolds number (Re)

Authors	Relationship	Comments
Test *et al.* (1981)	$h = 2.56V + 8.55$	Natural environment, V measured 1m above a 40^o inclined plate, flow remained laminar.
Sharples and Charlesworth (1998)	$h = 2.2V_r + 11.9$ ($0.5<V_r<6.7$) or $h = 9.1V_r^{0.57}$	1.8mx0.9m heated panel on windward 35^o pitch roof, 1-storey building. V_r was 1.5m above ridge.
Sparrow and Tien (1977)	$(h/\rho C_P V_\alpha)\, Pr^{2/3} = 0.931\, Re^{-1/2}$	Inclined and yawed square plate at a model scale. V_α is the free stream velocity measured upstream of the plate. Very low CHTC values c.f. full-scale data of Sharples and Charlesworth (1998).
Kind *et al.* (1983)	$h/\rho V_H C_P$ = f[Re] presented graphically.	Solar collector mounted on pitched roof of model house. V_H measured 14cm above the tunnel floor Very low CHTC values c.f. full-scale data of Sharples and Charlesworth (1998).
Clear *et al.* (2002)	$h = AV^{0.8} + B$ ($L>x_c$, A,B constant for constant temp. difference & geometry) $h = AV^{0.5} + B$ ($L<x_c$, A, B constant for constant temp. difference & geometry)	Horizontal roof. A, B = f(surface roughness, Re, Rayleigh (Ra), Prandtl (Pr) numbers), x_c =length of laminar region for forced convection, L=panel strip length. V at roof height.
Shao *et al.* (2009)	$h = 6.91V + 3.9$ (for $\Delta T>15^oC$ only)	Horizontal roof, 9-floor building, V at 1.6m above roof. Napthalene sublimation method
Kumar and Mullick (2010)	$h = (6.90 \pm 0.05) + (3.87 \pm 0.13)V$ or, $h = (6.63 \pm 0.05) + (3.87 \pm 0.13)V^{0.8}L^{-0.2}$	Flat plate mounted on horizontal roof. V at 0.15 m above the plate surface.
Loveday and Taki (1996)	$h = 2.00V_r + 8.91$ or $h = 16.15V^{0.397}$ (Proposed for wide building façades)	Windward wall panel, centre of 6th of 8-floor building, V_r at 11m above roof, V_s at 1m from panel.
Emmel *et al.* (2007).	$h = 5.15V^{0.81}$ (Windward wall) $h = 5.11V^{0.78}$ (Horizontal roof)	Isolated 8mx6mx2.7m low-rise building. 3D CFD steady RSM model. V at 10m height, 0° incidence
Blocken *et al.* (2009)	$h = 4.6V^{0.89}$ (Windward wall)	10m cube, 3D CFD steady RANS. R k-ε turbulence model. V at 10m height, 0° incidence.
Defraeye *et al.* (2010)	$h = 5.14V^{0.82}$ (Windward wall)	10m cube in ABL, 3D CFD steady RANS, R k-ε and SST k-ω turbulence models. Re varied. V at 10m height.

The review of the literature on CHTC modelling reveals a large variability in the reported correlations due to factors that include; (1) Different experimental building geometries (including roof slope), (2) Different approach flow (including mean velocity and turbulence), (3) Roof flows versus flat plate boundary layer flows, (4) Different Reynolds numbers (i.e. scale effects) and (5) Possibility of CHTC not being measured accurately or the value contains heat transfer associated with other mechanisms (i.e. radiation). There is clearly a lack of any study that focuses on the determination of convective heat transfer coefficient on an inclined roof of a low-rise building which

resembles the BIPV/T roof system. The review also shows that near-wall modelling is crucial in CHTC prediction; thus, the complete boundary layer should be modelled including the buffer and laminar sub-layer (Blocken *et al.*, 2009; Defraeye *et al.*, 2010; Ničeno *et al.*, 2002; Ratnam and Vengadesan, 2008).

The overall objective of the present research project is to evaluate the exterior CHTC on PV/T systems mounted on windward roof surfaces of low-rise buildings. The study focuses on geometries with roof slopes between 30° and 45° as these are known to result in optimal electrical and thermal efficiency for the BIPV/T system (Candanedo *et al.*, 2010; Chen, 2009). In this regard, a CFD approach is undertaken aiming to identify appropriate turbulence models that should be used to predict CHTC in this geometry, where the flow is expected to remain attached (for roof slopes higher than 40°) or the separated region is short (roof slopes around 30-35°). The paper describes 3-D steady and unsteady RANS simulations that have been performed to evaluate the wind flow field near the roof of a building with plan dimensions of 4.2 m by 6 m, 3 m roof height and 30° roof slope along with their validation using experimental data from a 1:50 scale model in a boundary layer wind tunnel. The paper also presents a parametric analysis for the windward roof CHTC by varying the eaves height Re ($1.3x10^5$ to $7.7x10^5$), using full-scale RANS simulations. A correlation is developed for exterior CHTC, using dimensionless parameters, and compared with results from previous full-scale experiments as well as with the boundary layer theory. This research is performed within the Canadian Solar Buildings Research Network and the specific building geometry was chosen to resemble that of a full-scale outdoor test-building (Candanedo *et al.*, 2010) with a roof-mounted PV/T system. Preliminary CFD simulations showed that exterior CHTC on the system is independent of the airflow through the BIPV/T channel and so the channel underneath the panels is not included in the work presented here.

2. EXPERIMENTAL SET-UP

The experiments were conducted in Boundary Layer Wind Tunnel (BLWT) II at the University of Western Ontario (working section of 3.4 m (width) x 2.5 m (height) x 39m length) at a relatively large geometric scale of 1:50, following previous work on low-rise buildings in the same facility, Kopp *et al.* (2005). The building model had plan dimensions of 12.00 cm by 8.32 cm, with a height of 6 cm and a 30^0 roof slope. The wind direction was normal to the windward façade, with a test speed of 10m/s (at z=1.45m) giving Re = $2x10^4$ based on wind speed at eaves height, and the model area blockage ratio was 0.12%. The undisturbed vertical profiles of mean wind speed and turbulence quantities were measured for 180 secs using crossed hot-wire anemometry at 60 kHz with the data low-pass filtered at 30 kHz. Centre-line vertical profiles of mean velocity (normalized by eave height velocity) and local turbulence intensity are shown in Figure 1, with the mean velocity fit by two log-law profiles (since a small internal boundary layer developed over the turntable). The first log-law, valid from the tunnel floor to 0.24m height, has $u_\tau/U_{EH} = 0.06$ and a roughness length, $z_0 = 0.06$ mm; where u_τ = frictional velocity (m/s), U_{EH} = velocity at eaves height (m/s). The second log-law, valid from 0.24m to 0.54m height, has $u_\tau/U_{EH} = 0.11$ and $z_0 = 2.5$ mm. Measurements of velocity profiles on the building centre-plane normal to the windward roof were taken at distances of s/S = 0, 0.2, 0.4, 0.6, 0.8 and 1 from the roof leading edge, where S is the total roof length (marked as "a" - "f" in Fig. 1).

3. NUMERICAL MODEL

A 3-D domain was used based on AIJ (Tominaga *et al.*, 2008), and COST (Franke *et al.*, 2007) guidelines (Fig. 2). Lateral and top boundaries were set at 5H from the building surfaces (H is the maximum height of the building), giving a blockage ratio of 2.1% which is smaller than the 3% noted in Franke *et al.* (2007). The distance between the inflow boundary and the building was 5H, with the outflow boundary at 15H downstream of the building to allow for wake flow redevelopment. In all cases the inflow direction was normal to the roof ridge. A finite volume method was used to generate the grid using GAMBIT 2.2.30. The whole building was nested by a rectangular block with a volume that was 3.5 times larger than the volume of the house. An unstructured tetrahedral mesh was generated inside the rectangular block, with prismatic cells on the walls, while a structured hexahedral mesh was used for the rest of the domain. Low Reynolds Number Modelling (LRNM), using the Realizable k-ε (R k-ε) and the Shear Stress Transport k-ω (SST k-ω) turbulence models, was used in the present work, an approach suggested by Blocken *et al.* (2009) but which requires very high grid resolution near the wall, compared to the wall function approach and so is computationally expensive. A dimensionless wall distance, $y^* = (C_\mu^{1/4} k_P^{1/2} y_P)/\mu$ or $y^+ = (u_\tau y_P)/\mu$, is used to characterize the grid resolution near the wall, where where, $C_\mu = 0.09$ in the wall-adjacent cells; k_P = turbulent kinetic energy at point P (m^2/s^2); y_P = distance of point P from the wall (m); u_τ = friction velocity (m/s). An

appropriate LRNM grid will have y* < 5 (Blocken *et al.*, 2009). On the surfaces of the building model a viscous boundary layer with 10 grid layers was generated with first cell height of 48μm for the model scale and 200μm for the full scale, giving the required y* values. A growth factor of 1.2 was used to generate the viscous sublayer. A grid independence study (G1 (coarse), G2 and G3 (finest)) showed that a grid with 1,376,389 cells (G2) provided sufficient resolution as the difference between the surface averaged CHTC values of the windward roof for G2 and G3 is within 1%. The refinement ratio between G1 and G2 was 1.6 in each dimension which is larger than the recommended value of 1.5 (Franke *et al.*, 2007; Tominaga *et al.*, 2008). However, the refinement ratio between G2 and G3 was limited to 1.3 by the available computational resources. The final grid and the mesh arrangements considered in this study are shown in Figure 2.

The velocity inlet boundary condition was used, with the two log-law equations imposed that matched the experimental mean velocity profile. The turbulent kinetic energy profile, based on the experimental values of the turbulent intensity, was also imposed at the inlet. Only forced convection heat transfer is considered in the

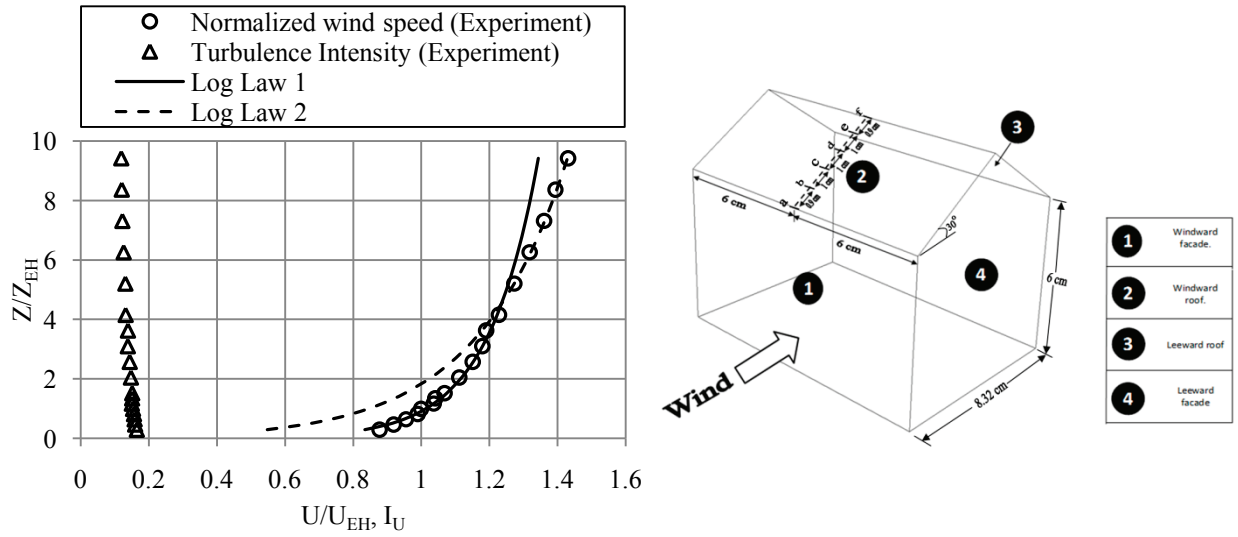

Figure 1: Vertical profiles of incident mean velocity (U/U_{EH}) and turbulence intensity (I_U) and locations of velocity measurements on windward roof

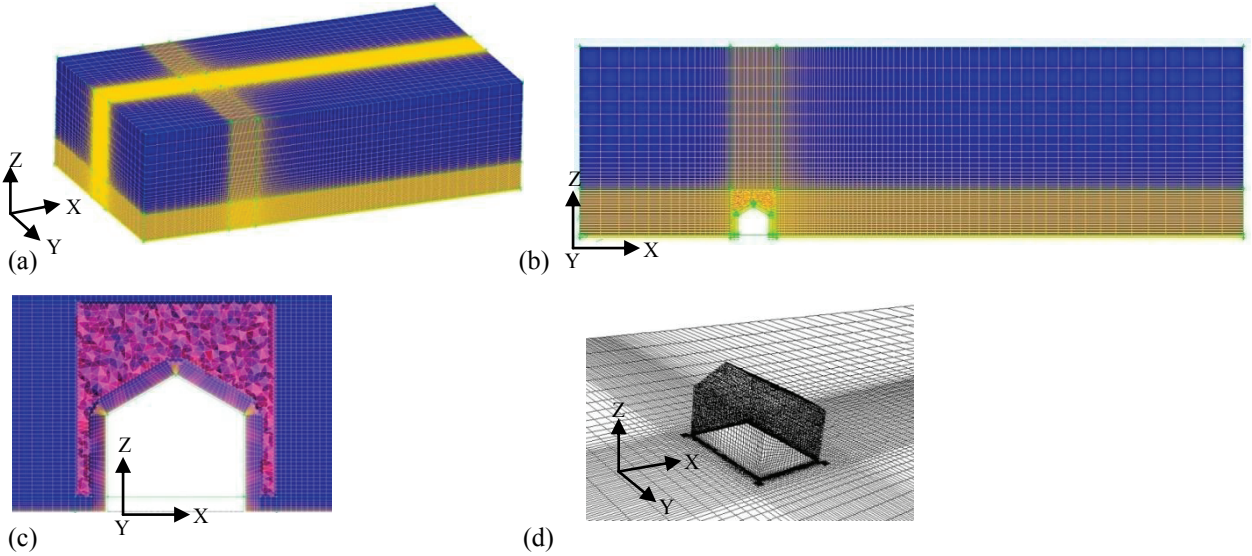

Figure 2: (a) Grid distribution on the entire domain; (b) Grid at the vertical mid-plane of the domain; (c) Grid at the vertical mid-plane near the building surfaces; (d) Grid on the building model and the bottom of the domain

simulation as the ratio of natural convection to forced convection, the Richardson Number, is much lower than unity (0.0042 at model scale). The thermal boundary conditions for the model were a fixed temperature of 313K (40°C) on the windward roof which is a typical PV temperature on a sunny winter day at Montréal, Canada (Candanedo *et al.*, 2010) and 263K (-10°C) at the inlet as well as for the reference temperature which also represents a typical winter condition in Montréal, Canada. All the walls of the house model and the bottom of the domain were treated as adiabatic. The air properties used in the simulations were density = 1.225 kg/m^3, dynamic viscosity = 1.7894x10^{-5} kg/m-s, thermal conductivity = 0.0242 W/m-K and specific heat capacity = 1006.43 J/kg-K. The CFD code FLUENT 6.3.26 was used to solve the equations with double precision. The second order discretization scheme was used throughout, except for the pressure interpolation which was Standard. For the pressure velocity coupling the SIMPLE algorithm was used. The convergence criterion for energy was 10^{-6} and for all other terms it was 10^{-4}.

LES models were developed during the initial phase of this research with the preliminary results (not shown here) demonstrating that a high resolution grid is needed not only in the wall normal direction but also in the streamwise direction (Cabot and Moin, 1999; Temmerman *et al.*, 2003), requiring substantial computing resources. A grid with a wall $y^*\approx1$, results in a high aspect ratio for the near-wall cells, since the cell length is necessarily much longer, which is unacceptable for LES but, as shown here, gives reasonable results when using RANS modelling. The initial LES results show how inappropriate near-wall modelling leads to a significant underestimation of CHTC. Correct near-wall modelling, especially in the laminar and buffer layer region, is very important as the heat transfer occurs in these regions (Defraeye *et al.*, 2010). DES (a hybrid LES/RANS scheme that employs an unsteady RANS (URANS) model in the near-wall region and LES elsewhere) is more computationally expensive than URANS alone but would not offer any improvement over the latter for the prediction of heat transfer on the windward roof since the LES model will not be activated there due to the absence of large eddies in that region. Therefore, in the present work URANS is performed with SST k-ω turbulence model and a time step size of 0.00015s. A total of 12 seconds of flow time was simulated and the average of the last 6 seconds was taken. The PISO algorithm was used for the pressure-velocity coupling and the same discretization scheme and convergence criteria as the steady state simulation.

4. RESULTS AND DISCUSSION

The mean velocity profiles on the windward roof using steady RANS with the R k-ε and SST k-ω turbulence models are compared with the experimental data in Figure 3 (a, b). For the R k-ε turbulence model, the predictions underestimate the experimental results (by up to 23%) at every location on the windward roof, although at most locations these underestimations are within 10%. Those points with a greater discrepancy are close to the roof leading edge and near the roof surface where the flow is highly unsteady. The SST k-ω model results indicate a better performance than with the R k-ε model, with the simulations being within 10% of the experimental data. Also as shown in Figure 3c, URANS gives similar results with the steady simulation; thus, a parametric analysis is carried out using steady RANS (with the SST k-ω turbulence model) for six different Reynolds numbers ($1.3x10^5$, $2.6x10^5$, $3.9x10^5$, $5.1x10^5$, $6.4x\times10^5$, $7.7x10^5$), based on wind speed at eaves height and roof length. At the inlet an atmospheric boundary layer velocity profile using the log law with z_0 = 0.03m, which represents grass covered terrain, and different wind velocities at 10 m height (1, 2, 3, 4, 5, 6 m/s) were used. In the simulations, the longitudinal turbulence intensity that is imposed at the inlet is based on the Engineering Science Data Unit (ESDU 83045) for z_0 = 0.03 m.

Using the results of the parametric analysis, the dimensionless heat transfer parameter Nusselt number (Nu) is correlated with the Reynolds numbers (Re) of the incoming flow. Here, Nu is calculated using the surface-averaged CHTC values of the windward roof and the roof length and Re is calculated using the wind velocity of the incoming flow at eaves height and the roof length. The correlation obtained is, $Nu = 0.11\ Re^{0.745}Pr^{1/3}$. Comparison of the predicted CHTC results with full-scale experimental data for a heated panel on windward 35° pitch roof (Sharples and Charlesworth, 1998) and a 40° inclined plate (Test *et al.*, 1981) is shown in figure 4(a). Since the plate length considered in various studies is different, the results of previous studies are normalized with respect to plate length

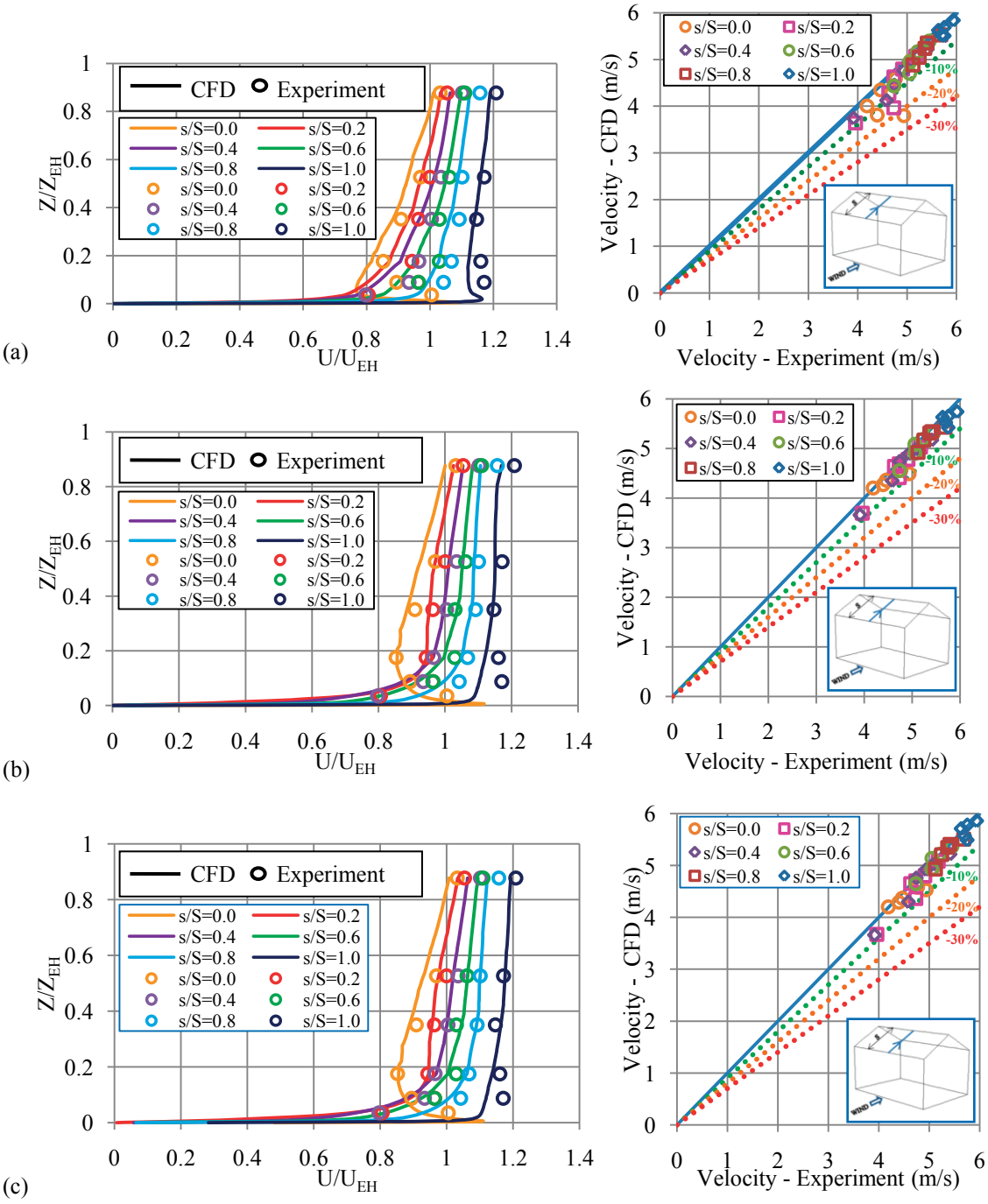

Figure 3: Mean velocity profiles along the mid-line of the windward roof; comparison between experimental data and CFD results using (a) SRANS R k-ε model (b) SRANS SST k-ω model (c) URANS SST k-ω model. Here, s is the distance from the leading edge and S is the total length of the roof.

of 2.4 m (using the relation $h \propto L^{-0.255}$ that is derived based on the above Nu number correlation) to make the comparison meaningful. The results were also normalized for the wind speed at eaves height considered in the present study by using $V_R/V_{EH} = 1.21$ for Sharples and Charlesworth (1998) and $V_R/V_{EH} = 1.19$ for Test *et al.* (1981) (V_R is the corresponding reference wind speed and V_{EH} is the wind speed at eaves height). Results presented in figure 4(a) show differences in the CHTC values when compared with those reported in previous studies with a

maximum difference of 24% with Sharples and Charlesworth (1998) and 29% with Test et al. (1981). These differences may be due to variations in the building geometries as well as the surroundings that make a direct comparison impossible. The results of the present study may also be compared with the correlation, $Nu = 0.036\ Re^{0.8}\ Pr^{1/3}$ (Incropera *et al.*, 2006) obtained from the boundary layer theory for turbulent flow over a horizontal flat plate (Fig. 4b). The wind speed at eaves height and the average CHTC values along the mid-line of the windward roof are used in the comparison. Figure 4 (b) illustrates that boundary layer theory under-predicts the CHTC values. This under-prediction is not surprising as the boundary layer theory was developed for uniform flow and without any free stream turbulence, the presence of which enhances heat transfer rates (Kondjoyan *et al.* 2002). Therefore, boundary layer theory alone should not be used to predict heat transfer where the flow is complex and free stream turbulence is present.

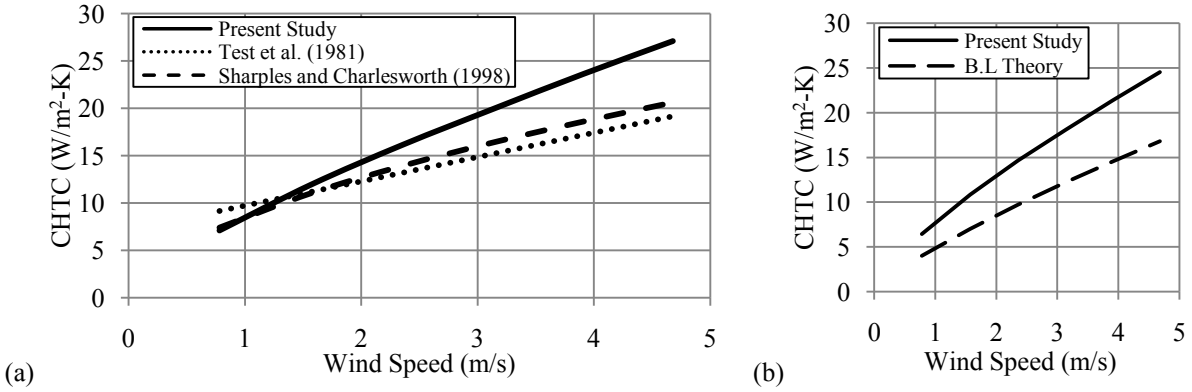

Figure 4: Comparison of present study with (a) previous studies (b) boundary layer theory.

5. CONCLUSIONS

CFD models have been developed to evaluate convective heat transfer coefficients (CHTC) on photovoltaic-thermal (PV/T) systems mounted on the windward roof of a low-rise building and validated with the results from a wind tunnel study on a 1:50 scale model. In general, the SST k-ω turbulence closure performed better than the R k-ε model in terms of matching the model-scale wind tunnel velocity profiles over the windward roof. A correlation has been developed for CHTC in terms of dimensionless parameters and compared with previous studies as well as with boundary layer theory. The results show that the boundary layer theory under-predicts the CHTC values significantly and should not be used alone to predict CHTC values in complex flows.

REFERENCES

Blocken, B., Defraeye, T., Derome, D. and Carmeliet, J., 2009, High-resolution CFD simulations for forced convective heat transfer coefficients at the façade of a low-rise building. *Building & Environment,* vol. 44: p. 2396-2412.

Cabot, W. and Moin, P., 1999, Approximate wall boundary conditions in the large-eddy simulation of high Reynolds number flow. Flow, *Turbulence and Combustion,* vol. 63: p. 269-291.

Candanedo,L., Athienitis, A.K., Candanedo, J., O'Brien, William, Chen, Y., 2010, Transient and steady state models for open-loop air-based BIPV/T systems. *ASHRAE Transactions*, In Press.

Chen, Y., 2009, Modeling and design of a solar house with focus on a ventilated concrete slab coupled with a BIPV/T System. Master's thesis, Dept of Building, Civil and Environmental Engineering, Concordia University.

Clear, R.D., Gartland, L. and Winkelmann, F.C., 2002, An empirical correlation for the outside convective air-film coefficient for horizontal roofs. *Energy and Buildings,* vol. 35: p. 797-811.

Defraeye, T., Blocken, B. and Carmeliet, J., 2010, CFD analysis of convective heat transfer at the surfaces of a cube immersed in a turbulent boundary layer. International Journal of Heat and Mass transfer vol. 53: p. 297-308.

Emmel, M.G., Abadie, M.O. and Mendes, N., 2007, New external convective heat transfer coefficient correlations for isolated low-rise buildings. *Energy and Buildings,* vol. 39: p. 335-342.

ESDU, 1983, Strong winds in the atmospheric boundary layer . Part 2: Discreet gust speeds. Engineering Science Data Unit Number 83045.

FLUENT 6.3 User's Guide, 2006. FLUENT Inc. Lebanon, New Hampshire, USA.

Franke, J., Hellsten, A., Schlünzen, H. and Carissimo, B., 2007, Best practice guideline for the CFD simulation of flows in the urban environment. COST Action 732; Quality assurance and improvement of microscale meteorological models.

Incropera, F. P., DeWitt, D. P., Bergman, T.L. and Lavine A. S., 2006, Fundamentals of Heat and Mass Transfer. 6th edition, John Wiley & Sons. New Jersey.

Kind R.J., Gladstone, D.H. and Moizer, A.D., 1983, Convective heat losses from flat-plate solar collectors in turbulent winds. *Transactions ASME, Journal Solar Energy Engineering,* vol. 105: p. pp 80-85.

Kondjoyan, A., Péneau, F. and Boisson, H. C., 2002, Effect of high free stream turbulence on heat transfer between plates and air flows: A review of existing experimental results. *International Journal of Thermal Sciences,* vol. 41, no. 1: p. 1-16.

Kopp, G. A., Surry, D. and Mans, C., 2005, Wind effects of parapets on low buildings: Part 1. Basic aerodynamics and local loads. *Journal of Wind Engineering and Industrial Aerodynamics,* vol. 93: p. 817-841.

Kumar, S. and Mullick, S.C., 2010, Wind heat transfer coefficients in solar collectors in outdoor conditions. *Solar Energy*, vol. 84: p. 956-963.

Loveday, D.L. and Taki, A.H., 1996, Convective heat transfer coefficients at a plane surface on a full-scale building façade. *International Journal of Heat and Mass Transfer,* vol. 39: p. 1729-1742.

Mullick, S.C., Kumar, S. and Chourasia, B.K., 2007, Wind induced heat transfer coefficient from flat horizontal surfaces exposed to solar radiation. In: Proceedings of Energy Sustainability 2007-ASME, June 27-30, Long Beach, California.

Ničeno, B., Dronkers, A.D.T. and Hanjalić, K., 2002, Turbulent heat transfer from a multi-layered wall-mounted cube matrix: a large eddy simulation. *International Journal of Heat and Fluid Flow,* vol. 23: p. 173-185.

Palyvos, J.A., 2008, A survey of wind convection coefficient correlations for building envelop energy systems modeling. *Applied Thermal Engineering,* vol. 28: p. 801-808.

Ratnam, G.S. and Vengadesan, S., 2008, Performance of two equation turbulence models for prediction of flow and heat transfer over a wall mounted cube. *International Journal of Heat and Mass Transfer,* vol. 51: p. 2834-2846.

Shao, J., Liu, J., Zhao, J., Zhang, W., Sun, D., and Fu, Z., 2009, A novel method for full-scale measurement of the external convective heat transfer coefficient for building horizontal roof. *Energy and Buildings,* vol. 41: p. 840-847.

Sharples, S. and Charlesworth, P.S., 1998, Full-scale measurements of wind induced convective heat transfer from a roof-mounted flat plate solar collector. *Solar Energy,* vol. 62: p. 69-77.

Sparrow, E.M. and Tien, K.K., 1977, Forced convection heat transfer at an inclined and yawed square plate - Applications to solar collectors. *Journal of Heat Transfer,* vol. 99, no. 4 : p. 507-512.

Temmerman, L., Leschziner, M. A., Mellen, C. P. and Fröhlich, J., 2003. Investigation of wall-function approximations and subgrid-scale models in large eddy simulation of separated flow in a channel with streamwise periodic constrictions. *International Journal of Heat and Fluid Flow,* vol. 24: p. 157-180.

Test, F. L., Lessmann, R.C., and Johary, A., 1981. Heat transfer during wind flow over rectangular bodies in the natural environment. *Transaction ASME Journal of Heat Transfer,* vol. 103: p. 262-267.

Tominaga, Y., Mochida, A., Yoshie, R., Kataoka, H., Nozu, T., Yoshikawa, M. and Shirasawa, T., 2008. AIJ guidelines for practical application of CFD to pedestrian wind environment around buildings. *Journal of Wind Engineering and Industrial Aerodynamics,* vol. 96: p. 1749-1761.

ACKNOWLEDGEMENT

This work was made possible by the support from the Natural Sciences and Engineering Research Council of Canada (NSERC) and the facilities of the Shared Hierarchical Academic Research Computing Network (SHARCNET: www.sharcnet.ca) and Compute/Calcul Canada. During this research Eric Savory was supported by the Region Pays de la Loire Visiting International Researcher program at the Ecole Centrale de Nantes, France. The authors would like to thank Mr. Luis Candanedo (PhD student, Concordia University) and Dr. William Lin (University of Western Ontario) for their valuable input.